# Modeling and Simulation of the Formation and Utilization of Microbial Products in Aerobic Granular Sludge

**Bing-Jie Ni and Han-Qing Yu**
Dept. of Chemistry, University of Science & Technology of China, Hefei, 230026 China

*DOI 10.1002/aic.11888*
*Published online September 15, 2009 in Wiley InterScience (www.interscience.wiley.com).*

*A mathematical model is established to simulate the formation of extracellular polymeric substances (EPS), soluble microbial products (SMP), and internal storage products ($X_{STO}$) in aerobic granular sludge. The sensitivity of these microbial products concentrations toward the key model parameters is analyzed. Independent experiments are conducted to find required parameter values and to test its predictive ability. The model is evaluated by using one-cycle operating experimental results of a lab-scale aerobic granule-based sequencing batch reactor (SBR) and batch experimental results. Results show that the model is able to describe the microbial product dynamics in aerobic granules and provide further insights into a granule-based SBR. The effect of the initial substrate and biomass concentrations on the formation of microbial products in aerobic granular sludge can therefore be analyzed by model simulation. A higher substrate concentration results in a greater concentration of EPS, SMP, and $X_{STO}$. An accumulation of biomass in the bioreactor leads to an increased production rate of EPS, SMP, and $X_{STO}$.* © 2009 American Institute of Chemical Engineers *AIChE J,* 56: 546–559, 2010

*Keywords: aerobic granular sludge, extracellular polymeric substances (EPS), soluble microbial products (SMP), storage polymers, modeling, sequencing batch reactor (SBR), wastewater treatment*

## Introduction

Recently, aerobic granule has been extensively investigated.[1–4] When compared with the conventional sludge flocs, the aerobic granules have a more compact structure, better settleability, and greater biomass retention. Studies have shown that the aerobic granule could be applied for high-strength organic wastewater treatment, simultaneous removal of organics matter, nitrogen, and phosphorus,[3] and toxic wastewater treatment.[5] Sequencing batch reactor (SBR) has been used for the granulation of activated sludge.[4,6] Aerobic-granule-based SBR has been proven to be applicable for the treatment of wastewaters from various industries, such as malting,[7] dairy,[8] and soybean-processing,[4] as well as municipal wastewater.[6] These results demonstrate that the aerobic granule has a great potential in municipal and industrial wastewater treatment.

Extracellular polymeric substances (EPS) are a major component of the matrix material in granules.[9,10] EPS are sticky solid materials secreted by cells, and they are involved in adhesion phenomena, formation of the matrix structure, controlling the microbial physiology, and the long-term stability of the granules.[10,11] In addition to EPS, all bacteria convert a fraction of the organic substrate into soluble microbial products (SMP), which account for the bulk of the soluble organic carbon in reactor effluents.[12–14] The incorporation of SMP formation has paved the way for more accurate modeling of biological wastewater treatment

Correspondence concerning this article should be addressed to H.-Q. Yu at hqyu@ustc.edu.cn

processes. On the other hand, the storage of the carbon sources as intracellular polymers, such as polyhydroxyalkanoates, lipids, and polysaccharides, is likely to play a significant role in the carbon turnover.[15–17] Aerobic granule SBR reactors are typically operated under highly dynamic conditions, attributed to the great substrate concentration gradients versus time.[15] As a result, microorganisms in granules experience alternative feast and famine conditions, which promote the occurrence of carbon storage. Microorganisms, which are capable of quickly storing substrate and consume this stored substrate in a more balanced way, have a strong competitive advantage over the microorganisms without such a capacity. As an essential intermediate, storage polymers play an important role in the overall substrate removal.

The EPS, SMP, and $X_{STO}$ are important sinks for electrons and carbon derived from the original substrate. The microorganisms in aerobic granules may promote the accumulation of $X_{STO}$, EPS, or both. For example, some microorganisms rapidly take up the external substrate and store it as $X_{STO}$ under feast conditions. The stored carbon is used for growth and maintenance in the subsequent famine period.[17] The carbon and electron sinking is important for the aerobic-granule-based reactors.[15]

Mathematical models are essential for optimizing design and improving operation of the complex biological processes.[18–20] Therefore, this article aims to elucidate the production and utilization of EPS, SMP, and $X_{STO}$ with a mathematical model. Furthermore, the work describes the mechanisms for the substrate removal of granules that have diffusion resistance for soluble components.[21] The sensitivity of these microbial products concentrations toward the key model parameters is analyzed using independent experiments. The model is evaluated by using one-cycle operation experimental results of a lab-scale aerobic granule-based SBR. Then, it is used to generate simulations about the effects of substrate and biomass concentrations on the dynamics of EPS, SMP, and $X_{STO}$ in aerobic-granule-based reactors.

## Materials and Methods

### *Reactor setup and operation*

Aerobic granules were cultivated in a laboratory-scale SBR, which had a working volume of 2 L with an internal diameter of 7.0 cm and a height of 100 cm. This SBR was operated sequentially as 3 min of influent filling, 227 min of aeration, 5 min of settling, and 5 min of effluent withdrawal. An air velocity of 0.4 $m^3\ h^{-1}$ was applied to the reactor, equivalent to a superficial upflow velocity of 2.8 $cm\ s^{-1}$. Effluent was drawn from the middle port of the reactor column, and the resulting hydraulic retention time (HRT) was 8 h. The SBR was fed with a fatty-acids-rich wastewater at a chemical oxygen demand (COD) of ~800 mg $L^{-1}$ and was operated at 20°C, resulting in a loading rate of 2.4 g COD $L^{-1}\ d^{-1}$ to the reactor. This wastewater was the effluent of a laboratory-scale anaerobic acidogenic reactor fed with sucrose-rich wastewater.[22] Butyrate, acetate, and propionate were its main constituents. In addition, 1.0 mL $L^{-1}$ of a microelement solution was added to the feed, which contained (in mg $L^{-1}$): $H_3BO_3$, 50; $ZnCl_2$, 50; $CuCl_2$, 30; $MnSO_4 \cdot H_2O$, 50; $(NH_4)_6M_{O7}O_{24} \cdot 4H_2O$, 50; $AlCl_3$, 50; $CoCl_2 \cdot 6H_2O$, 50; and $N_iCl_2$, 50. The influent pH value was adjusted to 7.0 through the dose of $NaHCO_3$ or HCl. The acidogenic effluent was diluted using tap water to obtain the influent to the SBR.

### *Parameter determination*

The substrate half-saturation coefficient ($K_S$) and endogenous-decay coefficient ($b_H$) were estimated as described by Henze et al.[23] The increase in maximum growth rate ($\mu_{H,S}$) with the increasing $S_S$ concentration in independent batch experiments was fitted to find the best-fit $K_S$ value. To estimate $b_H$, granules were removed from the SBR and put into an aerated batch reactor without feed. The $O_2$ respiration rate was measured at a given time interval over a period of several days. A plot of the logarithm of the respiration rate versus time gave a straight line with a slope $b_H$. The storage process parameters ($Y_{H,STO}$, $k_{STO}$, and $\mu_{H,STO}$) were estimated with the batch respirometry experiments. Before a respirometry test, the sludge was washed twice with distilled water to remove carry-over materials. Then, fatty-acids-rich wastewater was added as a pulse and the dissolved oxygen (DO) concentration was measured over time. The experiments were repeated with three different food-to-microorganism ratios for the parameters estimation. The initial substrate concentrations were set at 200, 300, and 400 mg COD $L^{-1}$, resulting in food-to-microorganism ratios of 0.2, 0.3, and 0.4 mg COD $mg^{-1}$ VSS, respectively. The calculated oxygen uptake rate (OUR) and measured COD variation were used for parameter estimation with the methods of Avcioglu et al.[24] The EPS and SMP formation parameters ($k_{EPS}$, $k_{UAP}$, and $k_{hyd}$) were estimated from the batch experimental results using aerobic granular sludge with the measurements of EPS and SMP under known initial conditions.

### *Batch experiments for model evaluation*

Independent sets of batch experiments under known initial conditions were conducted to evaluate the model. The aerobic granules were sampled from the SBR when substrate was depleted in the reactor. The sludge was kept under famine conditions and no internal storage products ($X_{STO}$) was formed inside it. After washed twice with distilled water to remove the external soluble organic material (SCOD), the granules were transferred to beakers with a working volume of 1 L. After that, the external substrate at predetermined concentrations was dosed, and the OUR was monitored until the substrate became depleted and the endogenous activity was resumed. Much different initial conditions from cycle operation were designed for model evaluation. Samples were taken every 10–20 min for the analysis of SCOD, EPS, SMP, and $X_{STO}$ (poly-beta-hydroxybutyrate, PHB).

### *Analytical procedures*

The DO concentration in the SBR was determined with a DO electrode (MO128, Mettler-Toledo Gmbh, Switzerland). Granules were conduct observed using an optical microscope (Olympus CX41). The granule size was measured using an image-analysis system (Image-pro Express 4.0, Media Cybernetics) with the Olympus CX41 microscope and a digital

camera (Olympus C5050). Determinations of COD, mixed liquor suspended solids (MLSS), and mixed liquor volatile suspended solids (MLVSS) followed the Standard Methods.[25]

The internal storage polymers, that is, poly-beta-hydroxybutyrate (PHB), were measured according to Pratt et al.[17] Samples of 10 mL were centrifuged at 4000 rpm for 10 min, decanted, and the biomass pellet freeze-dried at −54°C to remove the moisture content. The solid material was suspended in 2 mL of acidic methanol solution (3% $H_2SO_4$) and 2 mL of chloroform. The glass tube was screwed tightly and heated to 100°C for 6 h. After cooling, 1 mL of Milli-Q water was added to the tube and the resultant mixture was shaken vigorously for 10 min. When the phases were separated, 1 mL of the bottom organic layer was removed to the GC vials for PHB determination.

The SMP were determined according to Aquino et al.,[26] and the EPS were extracted as described by Wang et al.[27] Mixed liquid samples were centrifuged at 12,000 rpm for 15 min, and then were prefiltered through 0.45-$\mu$m acetate cellulose membranes to represent the SMP which was used for COD analyses. The EPS of the sludge samples were extracted using the cation exchange resin (CER) technique (Dowex Marathon C, 20–50 mesh, sodium form, Fluka 91973). Sludge samples were harvested by centrifugation at 3000 rpm for 15 min, and then the pellets were washed twice with 100 mM NaCl solution. After that the sludge pellets were resuspended to a predetermined volume and the solution was transferred to an extraction beaker, followed by the CER addition with a dosage of 60 g $g^{-1}$ SS. These suspensions were then stirred at 200 rpm and 4°C for 12 h. Afterwards, the CER/sludge suspensions were settled for 3 min to remove CER, and the EPS were harvested by centrifugation at 12,000 rpm and 4°C for 30 min to remove remaining sludge components. The supernatants were then filtrated through 0.45-$\mu$m acetate cellulose membranes and were used as the EPS fraction.

Transmission electron microscopy (TEM) analysis of PHB in the granules was performed according to Jendrossek et al.[28] The EPS distribution within the granules was examined using confocal laser scanning microscopy (CLSM) (LSM 5 Pascal, Zeiss, Jena, Germany). For florescent staining of both cells and EPS, two probes were applied collectively: SYTO9 (25 $\mu$m, Molecular Probe, Eugene, OR) to target all microbes, and ConA-TRITC lectin (250 mg $L^{-1}$, Sigma) to target the polysaccharides with D-glucose or D-mannose.

### *Mathematic modeling*

Modeling of a granule-based SBR involves oxygen transfer, diffusion within granules, and biological reactions. In this work, aerobic granules with a wide size of 0.41–3.5 mm are modeled with a consideration of substrate diffusion. The first step is its diffusion into the granules. Then, biological reactions involving each given model components occur within the granules.

A unified theory for EPS and SMP has been developed by Laspidou and Rittmann.[29,30] In this work, based on the unified model, a new model is established through introduction of simultaneous storage and growth concepts. Our model describes the relationships among the four solid species: active heterotrophic bacteria, EPS, $X_{STO}$, and residual inert biomass; three soluble species: external substrate and two unique forms of SMP; and an electron acceptor, which is dissolved oxygen. The model uses the following symbols for concentrations: external substrate ($S_S$), active heterotrophic biomass ($X_H$), internal storage products ($X_{STO}$), residual inert biomass ($X_I$), utilization-associated products ($S_{UAP}$), biomass-associated products ($S_{BAP}$), SMP ($S_{SMP} = S_{UAP} + S_{BAP}$), EPS ($X_{EPS}$), and DO ($S_O$). The units for all species are oxygen demand or oxygen (for DO), which is directly proportional to electron equivalents (8 g $O_2$ per $e^-$ equivalent).

The simultaneous storage and growth concepts are schematically shown in Figure 1. The external substrate is primarily used by active biomass $X_H$ for the generation of new biomass $X_H$. Excess amount of $S_S$ available is converted to $X_{STO}$. After the consumption of the primary external substrate, the secondary growth process occurs on the stored $X_{STO}$ in the famine phase.

Figure 2 illustrates the consistent approach for the fate of the substrate electrons, which directly enter a cell (i.e., active biomass primarily growth on $S_S$ in Figure 1). There are four possible ways. Part of the external substrate is used for biomass synthesis. Other substrate electrons are diverted to the formation of utilization-associated products (UAP) and EPS. UAP are released to the aqueous solution, whereas EPS are released as a solid to form the aggregate matrix. The hydrolysis of EPS produces biomass-associated products (BAP), which are soluble. Substrate oxidation and respiration of the electrons to reduce $O_2$ and generate the energy needed to fuel for formation of active biomass, EPS, and UAP. In our approach, the unified model is extended through the introduction of $X_{STO}$ formation and utilization. In a feast period, some of the external substrate is converted to $X_{STO}$. Because the formation of $X_{STO}$ competes with the usual biomass synthesis, the formation of $X_{STO}$ occurs only when the substrate concentration is high. The active biomass decays in two ways. First, the active biomass is oxidized through the endogenous respiration to yield energy for maintenance. Second, the decay also produces residual inert biomass, which is not biodegradable. Because both UAP and BAP are biodegradable, some of their electrons can also be used by the microorganisms as the ''recycled'' substrate, while the remaining electrons also go to the electron acceptor for energy generation. $X_{STO}$ is also biodegradable and can be utilized by the active biomass under the famine conditions. Some of the electrons in $X_{STO}$ are used for the biomass synthesis, while the other electrons are respired for energy generation. By convention,[12,13,29,30] the utilization of UAP, BAP, and $X_{STO}$ does not result in the formation of new UAP, EPS, or $X_{STO}$.

Related process kinetics and stoichiometry describing the interactions and transformations among model components are expressed in a way to be compatible with previous mathematical models, which have been proposed to formulate biochemical reactions of microbial populations fed with different types of substrate.[23,31] The structure of our model is presented in a matrix format reflecting the basic stoichiometric relationships constituting the backbone of the model.[23,31] The matrix format is outlined in Tables 1 and 2, where

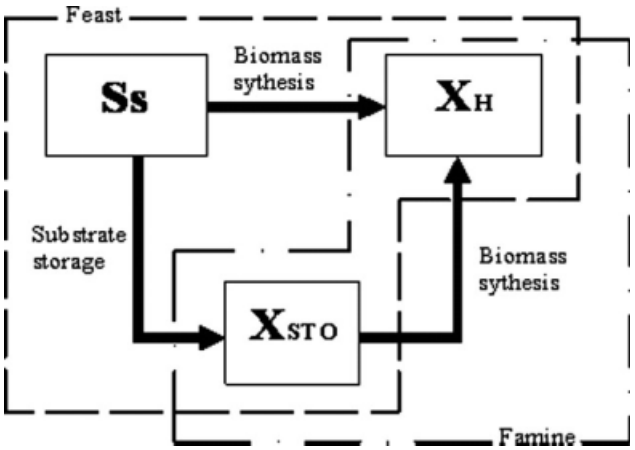


**Figure 1. Schematic diagram of the substrate utilization mechanisms for simultaneous growth and storage.**

model components are listed in the upper row; the rightmost column in Table 2 gives the process rate expressions; the relevant stoichiometric coefficients are incorporated in appropriate matrix cells. In this way, the generation or utilization rate in a model component for a given biochemical process is obtained by multiplication of related process stoichiometry and kinetics. Table 3 defines all the parameters, their units, and the values used in modeling and simulation results.

Modeling and simulation are performed using a software package AQUASIM,[32] a program designed mainly for parameter estimation and sensitivity analysis of the model. To simulate an aerobic-granule-based bioreaction process, the method of de Kreuk et al.[33] is adopted in this work. The model is integrated into the biofilm compartment of AQUASIM. The reactor in the model is described with a biofilm compartment connected to a mixed compartment with an advective link, and a high recirculation flow rate is incorporated from the biofilm compartment to the completely mixed one. The high recirculation rate is chosen to ensure the same concentrations in the liquor of biofilm compartment and the mixed compartment.[34] The biofilm compartment with a volume of 1 L contains the biomass granules and bulk liquid volume. The mixed compartment of 1 L includes the remaining liquor volume.[34]

In modeling the aerobic granules are assumed to be spherical in shape and their size distribution to be constant in one cycle of operation. A biofilm model implemented in AQUASIM is used to model the aerobic granules in this work.[35] One-dimensional conservation laws (Eq. 9) are formulated as a balance between the mass conserved and utilized in this granule model.[32]

$$\frac{\partial \hat{\rho}}{\partial t} + \frac{\partial \hat{j}}{\partial z} = \hat{r} \tag{1}$$

where $\hat{\rho}$ is the one-dimensional density (amount of conserved quantity per unit compartment length), $\hat{j}$ is the one-dimensional flux (amount of the conserved quantity transported per unit time), $\hat{r}$ is the one-dimensional source term (amount produced per unit compartment length and per unit time), $t$ is time, and $z$ is the space coordinate.

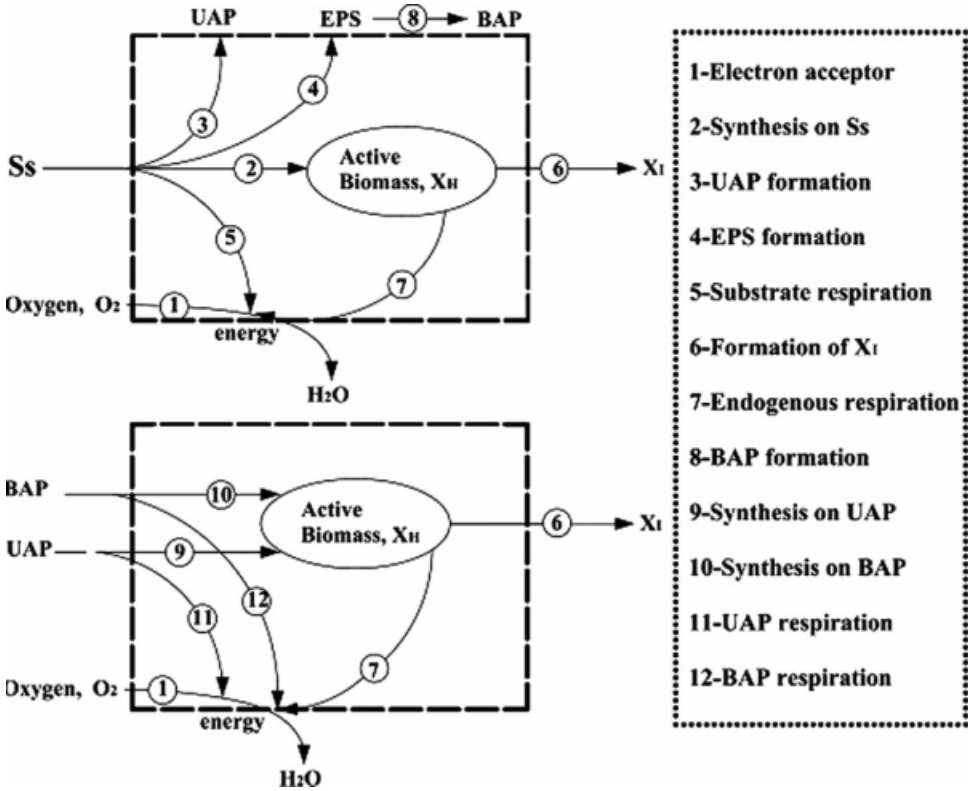


**Figure 2. Schematic diagram of electron flows regarding original substrate, active biomass, EPS, and SMP adapted from Laspidou and Rittmann (2002b).**

**Table 1. Stoichiometric Matrix for the Established Model**

| Component<br>Process | $S_O$<br>$O_2$ | $S_S$<br>COD | $S_{UAP}$<br>COD | $S_{BAP}$<br>COD | $X_I$<br>COD | $X_{EPS}$<br>COD | $X_H$<br>COD | $X_{STO}$<br>COD |
|---|---|---|---|---|---|---|---|---|
| Growth on $S_S$ | $-\frac{[1-k_{EPS}-k_{UAP}-k_{STO}-Y_{H,S}(1-k_{EPS}-k_{UAP}-k_{STO})]}{Y_{H,S}}$ | $-\frac{1}{Y_{H,S}}$ | $\frac{k_{UAP}}{Y_{H,S}}$ | | | $\frac{k_{EPS}}{Y_{H,S}}$ | $1-k_{UAP}-k_{EPS}-k_{STO}$ | $\frac{k_{STO}}{Y_{H,S}}$ |
| Growth on $X_{STO}$ | $-\frac{1-Y_{H,STO}}{Y_{H,STO}}$ | | | | | | 1 | $-\frac{1}{Y_{H,STO}}$ |
| Growth on $S_{UAP}$ | $-\frac{1-Y_{H,UAP}}{Y_{H,UAP}}$ | | $-\frac{1}{Y_{H,UAP}}$ | | | | 1 | |
| Growth on $S_{BAP}$ | $-\frac{1-Y_{H,BAP}}{Y_{H,BAP}}$ | | | $-\frac{1}{Y_{H,BAP}}$ | | | 1 | |
| Release of $X_{EPS}$ | | | | 1 | | $-1$ | | |
| Endogenous respiration | $-(1-f_I)$ | | | | $f_I$ | | $-1$ | |

The granules cultivated in this study had a size distribution between 0.41 and 3.5 mm with an average of 1.2 mm. It is true that granules with a wide range in size were formed in the reactor and that their size distribution also changed in time. However, the granule size distribution was not taken into account in this model, as it would significantly increase the complexity of numerical computation and it is not expected to contribute to a better understanding of the system. Therefore, in the simulation the diameter was chosen to be 1.2 mm, which was the most representative for the aerobic granules in this SBR. Because the experimental data measured in one cycle were different in time, depending on granule size, morphology, and reactor operation, a representative cycle measurement was selected to compare with a standard simulation case.[33] This simulation was performed under the same operational conditions as applied in the standard operation of the SBR. Parameters for the aerobic granules are shown in Table 4.

## Results and Discussion

### *Sensitivity to key model parameters*

Before the model calibration, sensitivity analysis should be conducted to evaluate the key parameters, which should be strictly kept under control in the experimental calibration and model validation. In the sensitivity analysis, the behavior of the model is evaluated as a consequence of a variation of the input parameters. The sensitivity coefficient represents the change in the output variable, resulting from a change in the input variable. Because the main purpose of this work is to simulate the dynamics of microbial products in the granular sludge, the output values of EPS, SMP, and $X_{STO}$ productions are analyzed. The sensitivity analysis results of key parameters are shown in Figures 3.

According to the simulation results in Figure 3, variation of $k_{EPS}$ (0.03–0.43 g $COD_{EPS}$ $g^{-1}$ $COD_S$) affects the EPS outcome significantly, while the change of $k_{STO}$ value from 0.03 to 0.43 g $COD_{STO}$ $g^{-1}$ $COD_S$ does affect the $X_{STO}$ outcome substantially. The parameter $k_{EPS}$ responsible for determining the EPS formation affects the outcome of SMP slightly, presumably attributed to the comparatively small amount of BAP, which are directly hydrolyzed from EPS. The $k_{STO}$ does not considerably influence the dynamics of SMP, because the utilizations of $X_{STO}$ does not result in the formation of new UAP. As shown in Figure 3, after an increase in the $k_{UAP}$ value from 0.02 to 0.10 g $COD_{UAP}$ $g^{-1}$ $COD_S$, the model predicts a much higher fraction of SMP, suggesting that $k_{UAP}$ should be a key parameter in the SMP formation. It also reveals that the UAP are the main SMP in the substrate utilization. When compared with $k_{EPS}$ and $k_{STO}$, the kinetic parameters $\mu_{H,STO}$ and $Y_{H,S}$ affect $X_{STO}$ slightly. With an increase in the $Y_{H,STO}$ value from 0.13 to 0.93 $h^{-1}$, the model predicts an increase in $X_{STO}$. The sensitivity analysis demonstrates that these key parameters have a great influence on the microbial product formation in the aerobic granular sludge.

### *Model calibration: parameter estimation with batch test results*

The parameter values are estimated by minimizing the sum of squares of the deviations between the measured data and the model predictions with the objective function given as below:

$$F(p) = \left( \sum_{i=1}^{n} (y_{exp,i} - y(p)_i)^2 \right)^{1/2} \quad (2)$$

where $y_{exp}$ and $y(p)$ are vectors of $n$ measured values and model predictions at times $t_i$ ($i$ from 1 to $n$), and $p$ is the vector of the model parameters.

To initiate the calibration procedure, an initial guess of the parameters is necessary. Such initial values are obtained with the experimental results and data in the literature. As shown in Table 3, parameters $b_H$ and $K_S$ were determined experimentally and independently, and were later used in the model. The initial concentration of active biomass was estimated using the baseline endogenous OUR level before substrate addition[36]:

**Table 2. Kinetics Rate Expressions for the Reaction Processes**

| Process | Kinetics Rate Expressions |
|---|---|
| Growth on $S_S$ | $\mu_{H,S} \frac{S_S}{K_S+S_S} \frac{S_O}{K_O+S_O} X_H$ |
| Growth on $X_{STO}$ | $\mu_{H,STO} \frac{K_S}{K_S+S_S} \frac{S_O}{K_O+S_O} \frac{X_{STO}/X_H}{K_{STO}+X_{STO}/X_H} X_H$ |
| Growth on $S_{UAP}$ | $\mu_{H,UAP} \frac{S_{UAP}}{K_{UAP}+S_{UAP}} \frac{S_O}{K_O+S_O} X_H$ |
| Growth on $S_{BAP}$ | $\mu_{H,BAP} \frac{S_{BAP}}{K_{BAP}+S_{BAP}} \frac{S_O}{K_O+S_O} X_H$ |
| Release of $X_{EPS}$ | $k_{hyd} X_{EPS}$ |
| Endogenous respiration | $b_H \frac{S_O}{K_O+S_O} X_H$ |

**Table 3. Kinetic and Stoichiometric Coefficients (20°C) for the Model**

| Parameter | Definition | Values | Unit | Reference |
|---|---|---|---|---|
| Stoichiometry | | | | |
| $Y_{H,S}$ | Yield coefficient for growth on $S_S$ | 0.39 | g $COD_X$/g $COD_S$ | This study (estimated) |
| $Y_{H,STO}$ | Yield coefficient for growth on $X_{STO}$ | 0.59 | g $COD_X$/g $COD_{STO}$ | This study (estimated) |
| $f_I$ | Fraction of $X_I$ in decay | 0.20 | g $COD_X$/g $COD_X$ | Gujer et al.[31] |
| $Y_{H,UAP}$ | Yield coefficient for growth on UAP | 0.45 | g $COD_X$/g $COD_{UAP}$ | Laspidou and Rittmann[30] |
| $Y_{H,BAP}$ | Yield coefficient for growth on BAP | 0.45 | g $COD_X$/g $COD_{BAP}$ | Laspidou and Rittmann[30] |
| Kinetics | | | | |
| $k_{STO}$ | $X_{STO}$ formation coefficient | 0.26 | g $COD_{STO}$/g $COD_S$ | This study (estimated) |
| $\mu_{H,STO}$ | Maximum growth rate on $X_{STO}$ | 0.51 | 1/h | This study (estimated) |
| $\mu_{H,S}$ | Maximum growth rate on $S_S$ | 0.40 | 1/h | Laspidou and Rittmann[30] |
| $K_S$ | Substrate affinity constant | 39.8 | g $COD_S/m^3$ | This study (measured) |
| $K_{STO}$ | Biomass affinity constant for $X_{STO}$ | 1.0 | g $COD_{STO}$/g $COD_X$ | Gujer et al.[31] |
| $K_O$ | Dissolve oxygen affinity constant | 0.2 | g $COD_O/m^3$ | Gujer et al.[31] |
| $b_H$ | Decay rate coefficient of $X_H$ | 0.035 | 1/h | This study (measured) |
| $k_{EPS}$ | EPS formation coefficient | 0.23 | g $COD_{EPS}$/g $COD_S$ | This study (estimated) |
| $k_{hyd}$ | EPS hydrolysis rate coefficient | 0.0071 | 1/h | Laspidou and Rittmann[30] |
| $k_{UAP}$ | UAP formation coefficient | 0.06 | g $COD_{UAP}$/g $COD_S$ | This study (estimated) |
| $\mu_{H,UAP}$ | Maximum rate of UAP degradation | 0.053 | 1/h | Laspidou and Rittmann[30] |
| $K_{UAP}$ | Biomass affinity constant for UAP | 100 | g $COD_{UAP}/m^3$ | Laspidou and Rittmann[30] |
| $\mu_{H,BAP}$ | Maximum rate of BAP degradation | 0.0029 | 1/h | Laspidou and Rittmann[30] |
| $K_{BAP}$ | Biomass affinity constant for BAP | 85 | g $COD_{BAP}/m^3$ | Laspidou and Rittmann[30] |

$$OUR_{end}(0) = (1 - f_I) \cdot b_H \cdot X_H(0) \quad (3)$$

In this equation, $f_I$ is fixed at 0.2 mg COD $mg^{-1}$ COD, as used in ASM3. Hence, for a given $f_I$ and measured $b_H$, $X_H(0)$ can be calculated from the $OUR_{end}(0)$ data. The model was first calibrated for the COD and OUR concentrations in the batch respirometric experiments. $Y_{H,STO}$, $k_{STO}$, and $\mu_{H,STO}$ were changed based on the causality of the parameters on the COD and OUR concentrations. The parameter values estimated are summarized in Table 3, whereas the simulation results are shown in Figure 4. The average absolute errors obtained are 9.5 mg $L^{-1}$ and 4.9 mg $L^{-1}$ $h^{-1}$ for COD and OUR concentrations, respectively. There is a good agreement between the model predictions and experimental data. Thereafter, the established model is also calibrated for the measured EPS and SMP concentrations in the batch experiments to determine an appropriate kinetics for simulating the dynamics of EPS and SMP in the aerobic granules. $k_{EPS}$, $k_{UAP}$, and $Y_{H,S}$ are changed based on the causality of the parameters on the EPS and SMP concentrations. The parameter values estimated are also listed in Table 3 with the simulation results are shown in Figure 5.

The calibrated heterotrophic maximum specific growth rate through the utilization of storage polymers ($\mu_{H,STO}$) is 0.51 1/h, which is slightly higher than the maximum specific growth rate for the external substrate ($\mu_{H,S}$) of 0.4 1/h. Thus, growth through the utilization of $X_{STO}$ is commensurate with growth on the external substrate. The $X_{STO}$ formation coefficient $k_{STO}$ is estimated to be 0.26 g $COD_{STO}$/g $COD_S$, while the EPS formation coefficient $k_{EPS}$ and the UAP formation coefficient $k_{UAP}$ are determined to be 0.23 g $COD_{EPS}$/g $COD_S$ and 0.06 g $COD_{UAP}$/g $COD_S$, respectively. Therefore, electrons from the external substrate are distributed in this order when $X_{STO}$ is produced: new biomass synthesis 39%, $X_{STO}$ 26%, EPS 23%, $O_2$ for respiration 6%, and UAP 6%. More substrate electrons are diverted to the storage polymers, but less is distributed to produce EPS and UAP when sufficient substrate is available. Considering the much higher utilization rate for $X_{STO}$ than that for UAP and BAP, the relatively higher distribution of electrons to $X_{STO}$ quantifies

**Table 4. Parameters for the Aerobic Granules in Model Simulation**

| Parameter | Description | Value | Reference |
|---|---|---|---|
| Granules | | | |
| $R_{min}$ | Minimum radius, mm | 0.41 | This study (measured) |
| $R_{max}$ | Maximum radius, mm | 3.50 | This study (measured) |
| $R_{mean}$ | Mean radius, mm | 1.20 | This study (measured) |
| *Mass transport* | | | |
| $D^{Ss}$ | Effective diffusivity of Ss, $dm^2$ $h^{-1}$ | 0.000576 | Beun et al.[34] |
| $D^{UAP}$ | Effective diffusivity of UAP, $dm^2$ $h^{-1}$ | 0.000576 | Beun et al.[34] |
| $D^{BAP}$ | Effective diffusivity of BAP, $dm^2$ $h^{-1}$ | 0.000576 | Beun et al.[34] |
| $D_{O2}$ | Effective diffusivity of $S_O$, $dm^2$ $h^{-1}$ | 0.0023 | Horn et al.[43] |
| Density of solid phase | | | |
| $\rho_{XH}$ | Density of $X_H$, g COD $m^{-3}$ | 35,000 | de Kreuk et al.[33] |
| $\rho_{XI}$ | Density of $X_I$, g COD $m^{-3}$ | 35,000 | de Kreuk et al.[33] |
| $\rho_{XSTO}$ | Density of $X_{STO}$, g COD $m^{-3}$ | 350,000 | de Kreuk et al.[33] |
| $\rho_{XEPS}$ | Density of $X_{EPS}$, g COD $m^{-3}$ | 4000 | Horn et al.[43] |

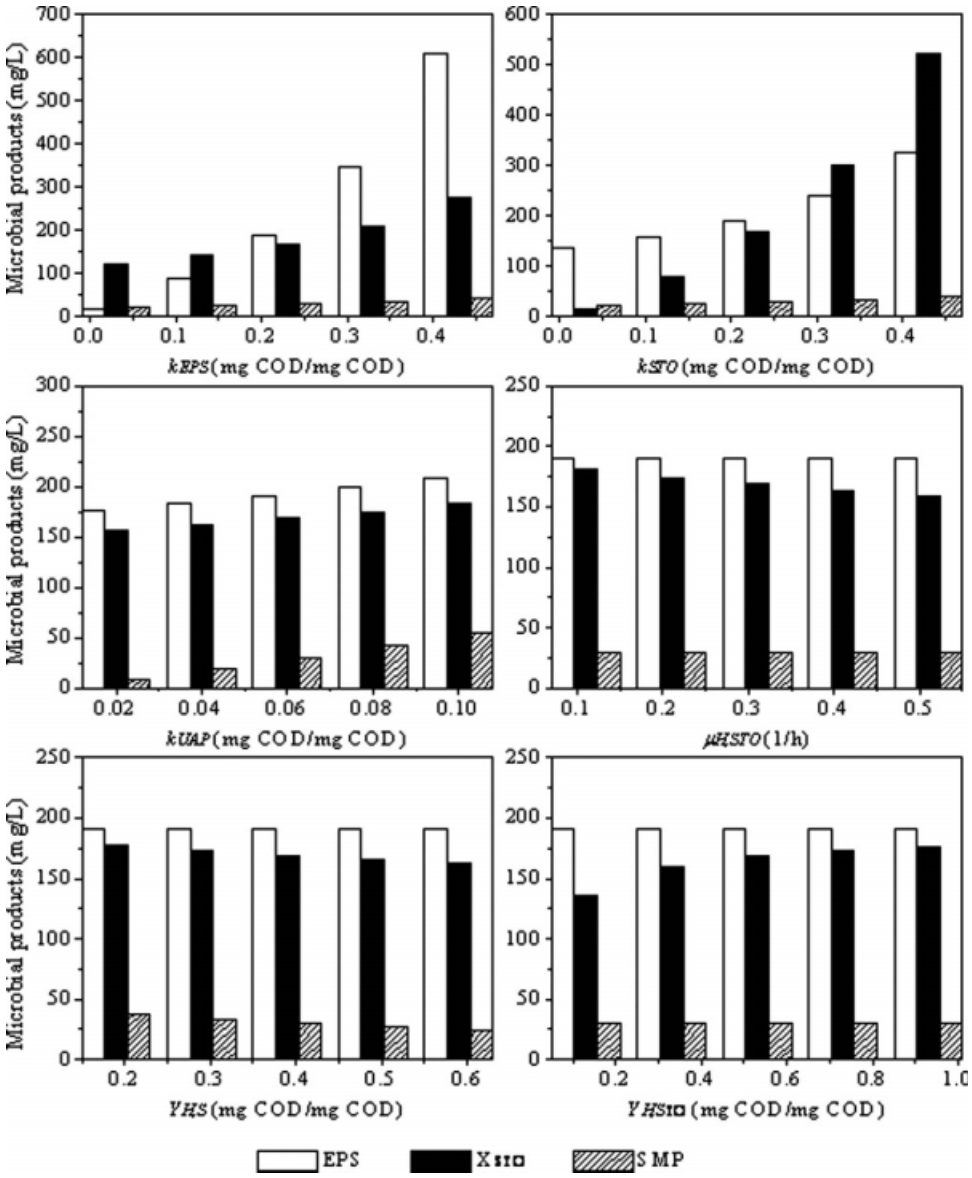


**Figure 3. Sensitivity analysis for the key model parameters: variation of EPS, SMP, and $X_{STO}$ productions with varied $k_{EPS}$, $k_{STO}$, $k_{UAP}$, $\mu_{H,STO}$, $Y_{H,S}$, and $Y_{H,STO}$ values.**

why $X_{STO}$ is the primary route by which the heterotrophs store the excess electrons and energy and later utilize them.

The yield coefficient for the growth on $X_{STO}$ is determined to be 0.59 g $COD_X$/g $COD_{STO}$, which is much lower than the value suggested by Gujer et al.,[31] partially attributed to the heterotrophic growth on the storage polymers rather than directly on the soluble substrates. Different model structure might be another reason for such a difference. The yield value for the utilization of the external substrate for microbial synthesis is relatively lower (0.39 g $COD_X$/g $COD_S$), when compared with the values reported in the literature,[17,23,31,36,37] because a significant amount of substrate electrons is diverted to the microbial storage products, rather than the active biomass. Furthermore, the EPS formation coefficient $k_{EPS}$ is higher than the value suggested by Laspidou and Rittman,[30] who estimated the parameters from a pure culture with chemostat experiment. Granular biomass is expected to have a significantly different physiology from this pure culture. The enhanced production of EPS observed for the aerobic granules is induced by some so-called stressful culture conditions.[38,39]

### *Model evaluation with the experimental data*

After one-month operation, aerobic granules became mature. They were yellow in color and spherical or ellipsoid in shape as shown in Figure 6A. The storage polymer production by the aerobic granules and the localization of the newly synthesized storage polymer were observed with TEM (Figure 6B). The TEM images reveal that the storage polymers with an electron-translucent globular structure are non-randomly distributed in the cell lumen, and that they are frequently found on or close to the cytoplasmic membrane. These internally accumulated storage polymers can then be

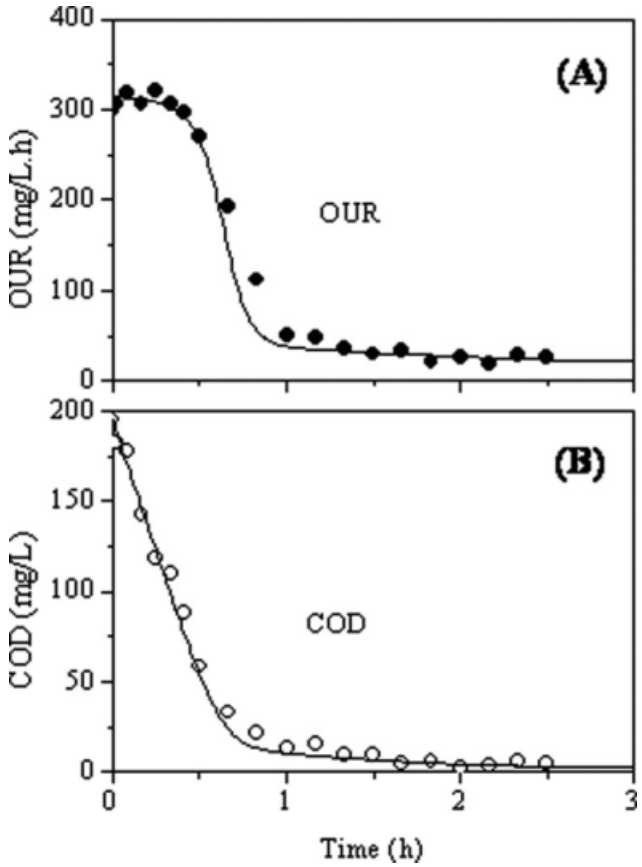


**Figure 4. Model calibration for the batch respirometric experimental data: (A) OUR profiles, and (B) COD measurements.**

utilized by microorganisms after the depletion of the added substrate. The CLSM examination after fluorescent staining indicates the EPS distributions in the aerobic granules. The EPS are nearly distributed uniformly throughout the whole granules (Figure 6C). The formation of aerobic granules is mainly attributable to the growth of cell together with the conglutination of EPS under hydrodynamic conditions. The substrate electrons are shuttled toward EPS production by the active microorganisms when they consume substrate electrons for their growth.

The model is solved for the set of parameters shown in Tables 3 and 4 in order to evaluate how well the model can describe the experimental results of the aerobic granule-based SBR. First, the independent data set for one-cycle operation of the SBR are simulated. The simulation results are shown in Figure 7, together with the measured OUR, $X_{STO}$, soluble COD (SCOD), and VSS concentrations in the laboratory-scale SBR during a cycle with the same operational conditions. The simulated OUR, $X_{STO}$, SCOD, and VSS profiles do not differ with values found in the experiments by more than 20%. Given all the uncertain parameters (e.g., exact granule size distribution and surface area), it is concluded that the model describes the experimental data well.

Secondly, Figure 8 shows the simulation and experimental results of OUR, SCOD, EPS, SMP, and $X_{STO}$ in a batch experiment, which are not used for model calibration. With the experimental measurements of EPS, SMP, and $X_{STO}$ in this batch experiment, the model ability to describe those microbial products can be tested directly. Furthermore, the initial conditions for this experiment are substantially different from those in Figure 7. The dosed external substrate (690 mg/L) is much higher than that of the cycling test (380 mg/L). The experimental trends, for example, the sharp decline of OUR, the peak of $X_{STO}$, and the leveling off of EPS after the depletion of the original substrate, and their absolute concentrations are described well by our model. The agreement between the model outputs and the measured data from different experiments supports that this model is able to properly describe the formation and utilization of the different types of microbial products in the aerobic granular sludge.

A tailing-off of the DO-consumption curve, which is observed in one cycle, can be appropriately described by the established model. Figures 7 and 8A show the simulation results for the predicted OUR profiles. The OUR initially increases, attributed to the rapid oxidation of the external substrate for growth and microbial product formation. The sharp bending point in the OUR corresponds with the complete removal of the dosed external substrate. The change of OUR is a direct indication of the transition from the feast phase to the famine phase, which occurs when the external substrate becomes depleted. The established model is able to

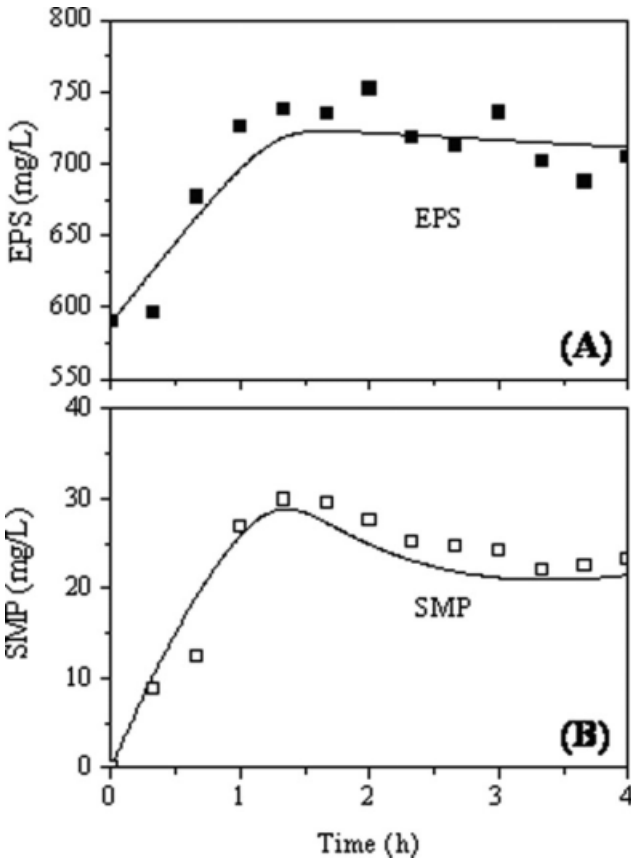


**Figure 5. Model calibration for the batch respirometric experimental data: (A) EPS data and (B) SMP concentrations.**

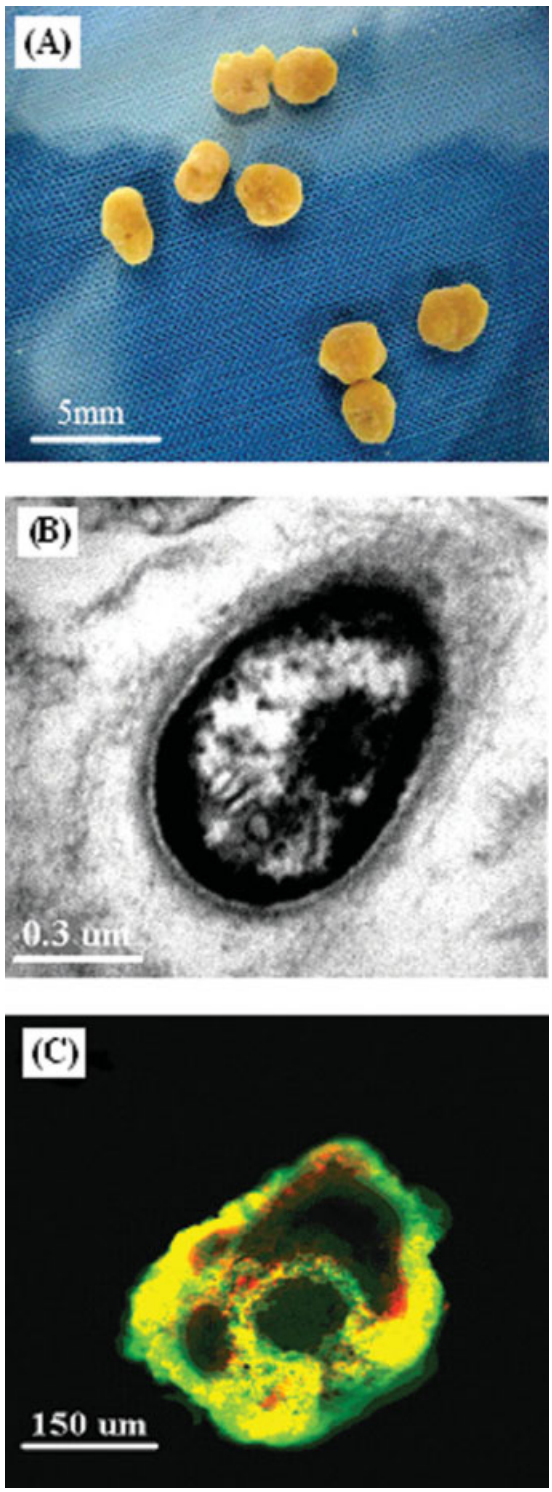


**Figure 6. (A) The image of the cultivated aerobic granules, (B) TEM analysis of the storage polymer granule produced within in aerobic granule, and (C) CLSM images of the 50-$\mu$m cryosections through the center of the aerobic granule.**

Cells are stained with SYTO9 (green) and polysaccharides are stained with ConA (red). [Color figure can be viewed in the online issue, which is available at www.interscience.wiley.com.]

predict both initial OUR response and smooth transition to the famine phase. However, the OUR does not immediately return to the endogenous respiration level because of the oxidation of $X_{STO}$ and SMP, which are formed when the external substrate is being utilized.

The model is also verified with the SCOD and storage polymer data (Figures 7 and 8B). Attributed to the initial rapid storage and consumption of substrate by the heterotrophs, the SCOD is reduced sharply at the initial stage. However, a complete depletion of the soluble COD does not occur because of the SMP formation (Figure 8E). Furthermore, the measured biomass (VSS) variations match with the model predictions. The VSS initially increases from 800 to 1200 mg $L^{-1}$, and later gradually decreases to 1100 mg $L^{-1}$ (Figure 7D). In the period of rapid growth, both $X_{STO}$ and EPS (Figure 8F) increase rapidly and occupy a significant fraction of total VSS. However, once $S_S$ is consumed and the rapid growth ceases, only $X_{STO}$ is rapidly utilized to provide for new synthesis with a relatively high rate under famine conditions. Thus, in the period of net biomass decay, the EPS and $X_H$ become the main fractions of total VSS, while the $X_{STO}$ fraction declines (Figure 8). There is a good agreement between the model outputs and experimental data of the aerobic granule SBR, demonstrating the validity of the model established in this article.

The concepts behind the developed model and the modeling approach shown here quantify the interconnections of EPS, SMP, and $X_{STO}$ and offer a new integrated framework to describe these concepts with mathematical expressions and complete mass balances. Ahn et al. established a model by incorporating the unified EPS and SMP concept into the membrane bioreactor process based on ASM1 in order to predict their fates under various SRT conditions.[40] With their model, EPS and SMP production could be simulated well and the results could be applied for the membrane bio-fouling control. In the unified theory of Laspidou and Rittmann,[29,30] the hydrolysis of EPS was assumed to be the sole source of BAP. However, there are some disagreements in the literature regarding the unified theory.[41] In addition to the soluble EPS, there are other BAP that might be released into the bulk solution as a result of lysis (i.e., endogenous organics and cell debris) and cell maintenance (i.e., turnover of intracellular components). Aquino and Stuckey proposed that both soluble EPS and cell lysis products are the sources of BAP.[41] In addition, soluble intracellular components may end up in the bulk solution because of the renewal and turnover of the internal structures or as a result of survival strategies adopted by microorganisms.[26] Ramesh et al. compared the physicochemical characteristics of the SMP and soluble EPS from different sludge samples and concluded that that SMP are not identical to the soluble EPS.[42] Because of the complexity of the microbial processes and the difficulty in modeling, information about the BAP formation is still sparse. There are also controversial reports about the BAP mechanisms in previous studies.[29,30,41,42] Because no experimental method is available to accurately quantify the real source of BAP, the model of Laspidou and Rittmann is adopted in our work.[29,30] Furthermore, when compared with the approach of Beun et al.,[34] in our work, the biomass growth and $X_{STO}$ formation kinetics are integrated into one overall reaction, in which biomass and storage product are

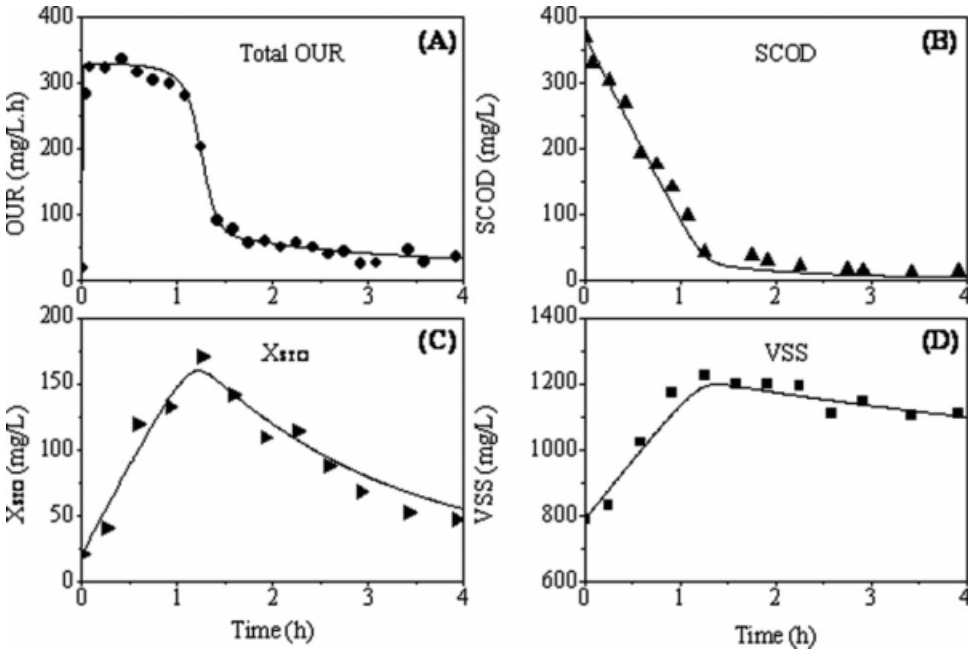


**Figure 7. Model evaluation of OUR profiles, $X_{STO}$ data, soluble COD data, and VSS profiles during one-cycle operation of the aerobic granule-based SBR (Line for model simulation and dot for measured data).**

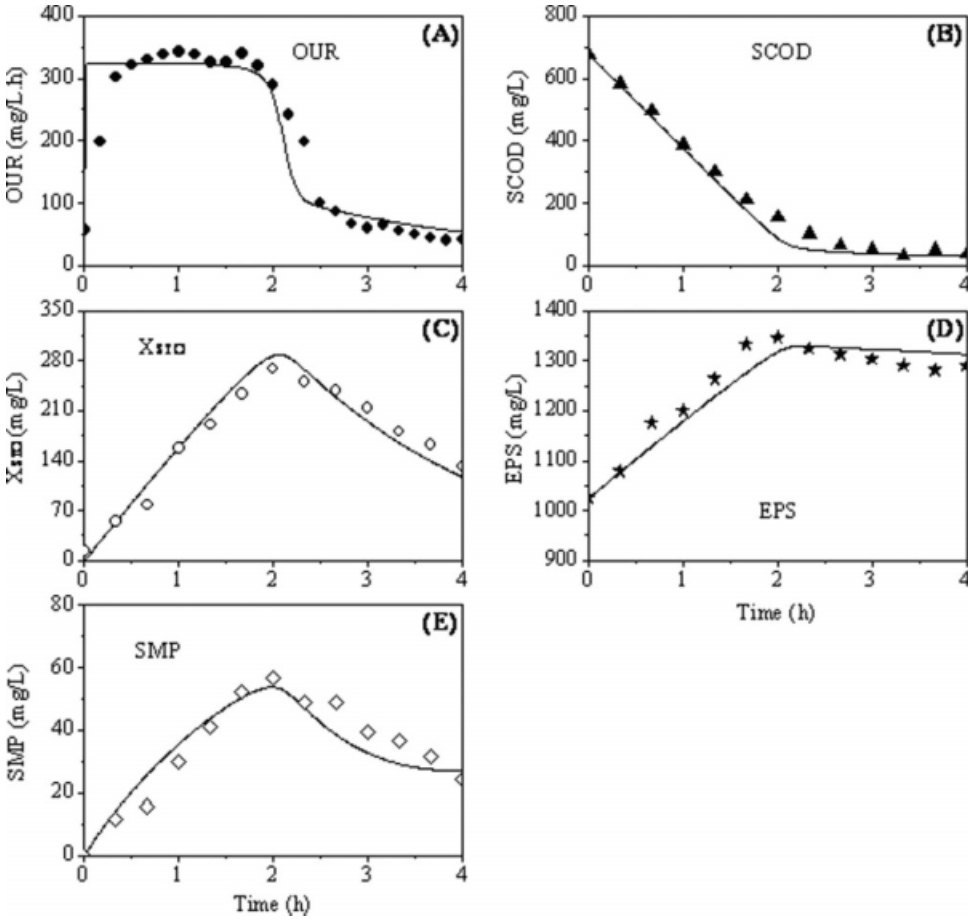


**Figure 8. Model evaluations of the OUR, $X_{STO}$, SCOD, EPS, and SMP profiles in batch experiments (Line for model simulation and dot for measured data).**

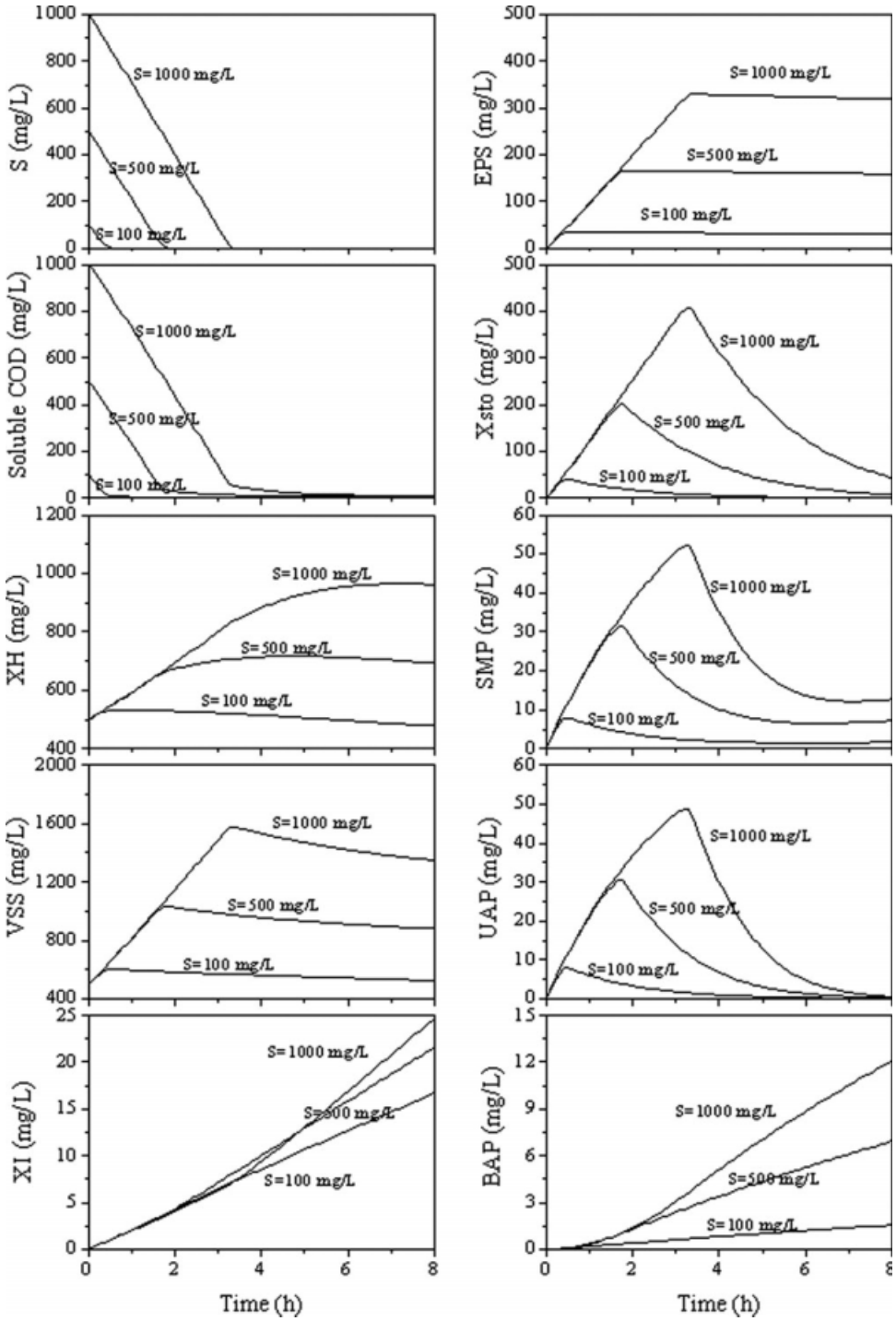


**Figure 9. Effect of the substrate concentration on $S_S$, SCOD, active biomass, VSS, $X_I$, EPS, $X_{STO}$, SMP, UAP, and BAP profiles.**

produced. In this way, the formation of $X_{STO}$ is coupled with the energy generation and respiration, and the $X_{STO}$ formation rate is proportional to the substrate utilization rate. For aerobic granule systems, the model incorporating EPS, SMP, and $X_{STO}$ formation and degradation may offer a rational approach to describe the bioreactor process. The new model provided here would be useful for the design, development, and application of the aerobic granular sludge process.

### *Effect of substrate concentration on EPS, SMP, and $X_{STO}$*

The effect of the influent substrate concentration on the model components is investigated with the parameters in Tables 3 and 4. Figure 9 shows the model predicted profiles of $S_S$, soluble COD, $X_H$, MLVSS, $X_I$, EPS, $X_{STO}$, SMP, UAP, and BAP in an aerobic-granule-based reactor. A higher substrate concentration results in a greater concentration of

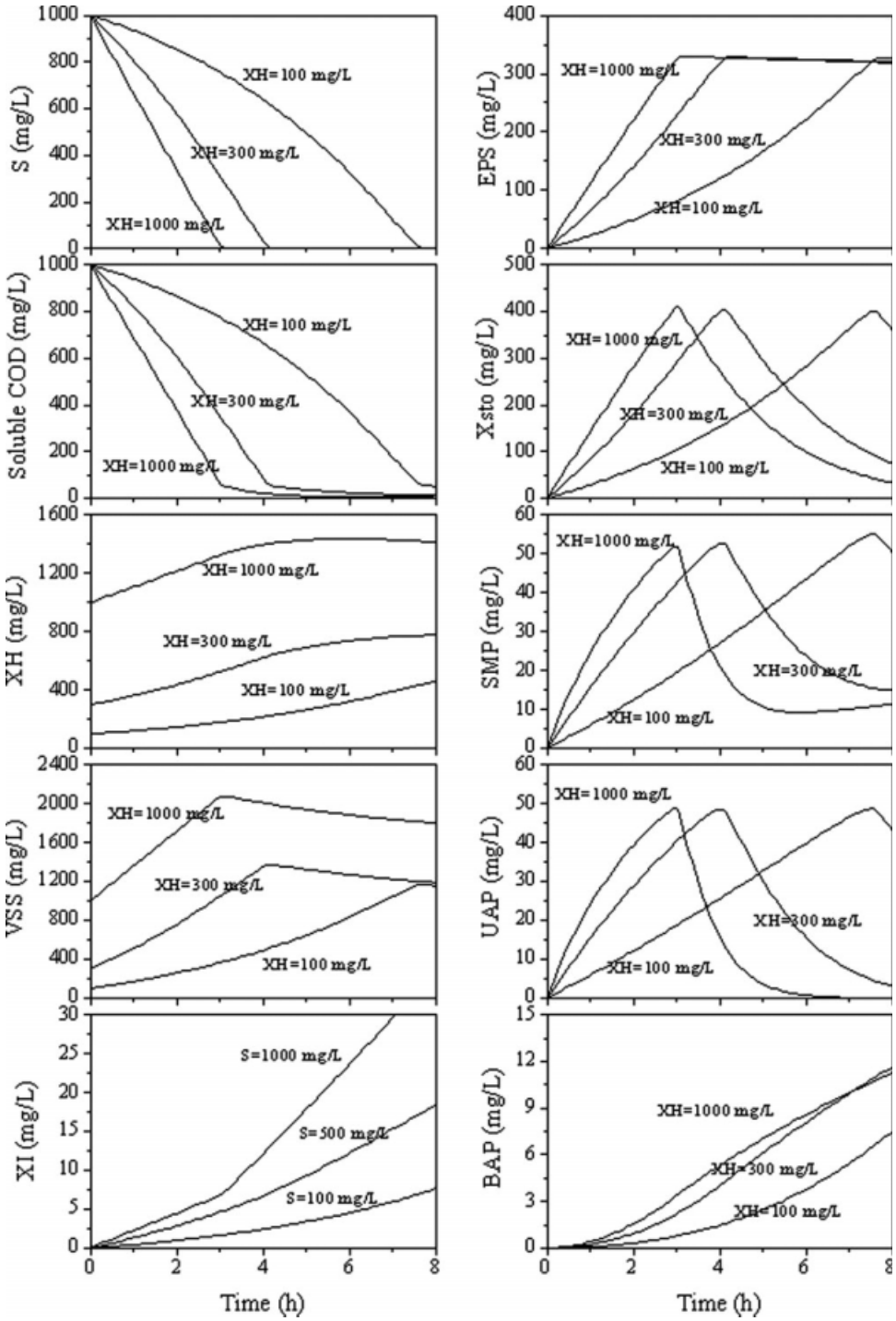


**Figure 10. Effect of the biomass concentration on $S_S$, SCOD, active biomass, VSS, $X_I$, EPS, $X_{STO}$, SMP, UAP, and BAP profiles.**

EPS, $X_{STO}$, and $X_H$. The EPS and $X_{STO}$ dependence on the substrate concentration is attributed to the fact that $S_S$ governs the substrate utilization rate ($r_S X_H = \frac{\mu_{H,S}}{Y_{H,S}} \frac{S}{K_S+S} \frac{S_O}{K_{O2}+S_O} X_H$), and accordingly the EPS and $X_{STO}$ formation rate. UAP increases with the increasing substrate concentration, attributed to the same mechanisms for the EPS formation. Both BAP and $X_I$ increase with an increase in substrate concentration, because the "parent" compounds, that is, EPS and active biomass, increase with the increasing $S_S$. Thus, a higher initial $S_S$ generates a greater level of total SMP (UAP + BAP). With the increasing $X_H$, $X_I$, EPS, and $X_{STO}$, the VSS also increases with the increasing substrate concentration (Figure 9). These results clearly demonstrate the role of influent substrate concentration in the formation of EPS, SMP, and $X_{STO}$ in the aerobic granular sludge.

At a higher influent substrate concentration, all reactions in a bioreactor will last longer. This has a significant influence on the SBR performance. In an operating cycle of an SBR, the UAP concentration rapidly decreases in a long cycle time, with a low production rate ($k_{UAP}r_S X_H$), but its degradation rate does not decline significantly. Thus, the UAP are a major component in the effluent only when the cycle time is relatively short. On the contrary, the BAP are the most important component in the effluent when the cycle time is long. In both cases, a high influent $S_S$ would increase the effluent soluble COD concentration in each cycle. For a long cycling time, the EPS become a large fraction of total VSS, in addition to $X_H$. For a short cycle period, the $X_{STO}$ occupy a great fraction of total VSS. Moreover, $X_I$ builds up continually. As a result, the increasing content of EPS, $X_{STO}$, and $X_I$ would decrease the active biomass fraction of the total VSS. Hence, it is important to optimize a bioreactor operated at a high influent substrate concentration, in order to avoid a high effluent soluble COD (UAP and BAP) level as well as an accumulation of a high amount of nonactive biomass (EPS, $X_{STO}$, and $X_I$), and also to reduce the associated high operating costs.

### *Effect of biomass concentration on EPS, SMP, and* $X_{STO}$

The formation of EPS, SMP, and $X_{STO}$ has been shown to be closely linked to the quantity of active biomass present in a bioreactor. The EPS, SMP, and $X_{STO}$ are produced at a rate proportional to the active biomass concentration, for instance, the EPS formation $= k_{EPS}r_S X_H$. Hence, an accumulation of active biomass in the bioreactor leads to an increased production rate of EPS, SMP, and $X_{STO}$. This is confirmed by the simulation results in this work. Figure 10 shows the model predictions for $S_S$, soluble COD, $X_H$, MLVSS, $X_I$, EPS, $X_{STO}$, SMP, UAP, and BAP profiles at three different active biomass concentrations. The EPS, UAP, BAP, and $X_{STO}$ concentrations reach their peak values more rapidly at a higher biomass concentration. The production rates of EPS, SMP, and $X_{STO}$ by the granular sludge increase with an increase in biomass concentration. The total $X_I$ and BAP content increases with an increase in biomass concentration. The total content of EPS, UAP, and $X_{STO}$, however, does not show a direct correlation with the active biomass concentration. A lower active biomass concentration is not responsible for the lower concentration of EPS, UAP, and $X_{STO}$. In addition to the biomass concentration, as mentioned above, the substrate concentration is an important factor governing the production of these organic materials by microorganisms.

For an application point of view, a higher level of active biomass would enhance the effluent quality at a given HRT. The external substrate removal rate increases with the increasing active biomass content. A higher active biomass concentration would not result in a higher UAP content in the reactor (Figure 10). Therefore, the effluent soluble COD concentration would decrease. Furthermore, a higher active biomass concentration would not result in a higher content of EPS and $X_{STO}$, but would increase the active biomass fraction of the total VSS.

## Conclusions

The model established in this work describes the formation and utilization of microbial products, such as EPS, SMP, and $X_{STO}$, in an aerobic-granule-based bioreactor. The model simulates the experimental data from this complex system sufficiently well, as the simulated trends in OUR, EPS, SMP, $X_{STO}$, soluble COD, and VSS are similar to those measured in the experiments. Simulation results underline the importance of the initial substrate and biomass concentrations for the overall formation and consumption of EPS, SMP, and $X_{STO}$ in the aerobic granules. A higher substrate concentration results in a greater concentration of EPS, SMP, and $X_{STO}$. An accumulation of biomass in a bioreactor leads to an increased production rate of EPS, SMP, and $X_{STO}$. However, there is no direct correlation between the biomass concentration with the total content of the EPS, SMP, and $X_{STO}$. The model can be used for process understanding and thus for optimization of the aerobic-granul-based reactors.

## Acknowledgments

The authors wish to thank the Natural Science Foundation (NSFC) of China (20577048, 50625825, 50708106 and 50738006) for the partial support of this study.

## Literature Cited

1. Peng D, Bernet N, Delgenes JP, Moletta R. Aerobic granular sludge-a case study. *Water Res.* 1999;33:890–893.
2. Beun JJ, van Loosdrecht MCM, Heijnen JJ. Aerobic granulation in a sequencing batch airlift reactor. *Water Res.* 2002;36:702–712.
3. de Kreuk K, Heijnen JJ, van Loosdrecht MCM. Simultaneous COD, nitrogen, and phosphate removal by aerobic granular sludge. *Biotechnol Bioeng.* 2005;90:761–769.
4. Su KZ, Yu HQ. Formation and characterization of aerobic granules in a sequencing batch reactor treating soybean-processing wastewater. *Environ Sci Technol.* 2005;39:2818–2827.
5. Jiang HL, Tay JH, Tay STL. Aggregation of immobilized activated sludge cells into aerobically grown microbial granules for the aerobic biodegradation of phenol. *Lett Appl Microbiol.* 2002;35:439–445.
6. de Kreuk MK, van Loosdrecht MCM. Formation of aerobic granules with domestic sewage. *J Environ Eng.* 2006;132:694–697.
7. Schwarzenbeck N, Erley R, McSwain BS, Wilderer PA, Irvine RL. Treatment of malting wastewater in a granular sludge sequencing batch reactor (SBR). *Acta Hydrochim Hydrobiol.* 2004;32:16–24.
8. Arrojo B, Mosquera-Corral A, Garrido JM, Mendez R. Aerobic granulation with industrial wastewater in sequencing batch reactors. *Water Res.* 2004;38:3389–3399.
9. McSwain BS, Irvine RL, Hausner M, Wilderer PA. Composition and distribution of extracellular polymeric substances in aerobic flocs and granular sludge. *Appl Environ Microbiol.* 2005;71:1051–1057.
10. Sheng GP, Yu HQ, Li XY. Stability of sludge flocs under shear conditions: roles of extracellular polymeric substances (EPS). *Biotechnol Bioeng.* 2006;93:1095–1102.
11. Tay JH, Liu QS, Liu Y. The effects of shear force on the formation, structure and metabolism of aerobic granules. *Appl Microbiol Biotechnol.* 2001;57:227–233.
12. de Silva DGV, Rittmann BE. Interpreting the response to loading changes in a mixed-culture completely stirred tank reactor. *Water Environ Res.* 2000;72:566–573.
13. de Silva DGV, Rittmann BE. Nonsteady-state modeling of multispecies activated-sludge processes. *Water Environ Res.* 2000;72:554–565.
14. Magbanua BS Jr, Bowers AR. Characterization of soluble microbial products (SMP) derived from glucose and phenol in dual substrate Activated Sludge Bioreactors. *Biotechnol Bioeng.* 2006;93:862–870.

15. van Loosdrecht MCM, Pot M, Heijnen J. Importance of bacterial storage polymers in bioprocesses. *Water Res.* 1997;35:41–47.
16. Majone M, Dircks K, Beun J. Aerobic storage under dynamic conditions in activated sludge processes-The state of the art. *Water Sci Technol.* 1999;39:61–73.
17. Pratt S, Yuan Z, Keller J. Modelling aerobic carbon oxidation and storage by integrating respirometric, titrimetric, and off-gas $CO_2$ measurements. *Biotechnol Bioeng.* 2004;88:135–147.
18. Lee TT, Wang FY, Newell RB. Distributed parameter approach to the dynamics of complex biological processes. *AIChE J.* 1999;45: 2245–2268.
19. Ajbar A, Alhumazi K. Microbial competition: study of global branching phenomena. *AIChE J.* 2000;46:321–334.
20. Nopens I, Koegst T, Mahieu K, Vanrolleghem PA. PBM and activated sludge flocculation: from experimental data to calibrated model. *AIChE J.* 2005;51:1548–1557.
21. Beyenal H, Leker L, Tanyol A. Diffusion coefficients of phenol and oxygen in a biofilm of pseudomonas putida. *AIChE J.* 1997;43:243–250.
22. Mu Y, Yu HQ. Biological hydrogen production in a UASB reactor with granules I: physicochemical characteristics of hydrogen-producing granules. *Biotechnol Bioeng.* 2006;94:980–987.
23. Henze M, Grady CPL Jr, Gujer W, Marais GVR, Matsuo T. Activated sludge model No. 1. *Scientific and Technical Report No.* 1, 1987, IAWPRC, London.
24. Avcioglu E, Karahan G, Orhon D. Estimation of stoichiometric and kinetic coefficients of ASM3 under aerobic and anoxic conditions via respirometry. *Water Sci Technol.* 2003;48:185–194.
25. APHA. *StandardMethods for the Examination of Water and Wastewater*, 19th ed. Washington, DC: American Public Health Association, 1995.
26. Aquino SF, Stuckey DC. Soluble microbial products formation in anaerobic chemostats in the presence of toxic compounds. *Water Res.* 2004;38:255–266.
27. Wang J, Yu HQ. Biosynthesis of polyhydroxybutyrate (PHB) and extracellular polymeric substances (EPS) by *Ralstonia eutropha* ATCC 17699 in batch cultures. *Appl Microbiol Biotechnol.* 2007;75:871–879.
28. Jendrossek D, Selchow O, Hoppert M. Poly(3-hydroxybutyrate) granules at the early stages of formation are localized close to the cytoplasmic membrane in *Caryophanon latum*. *Appl Environ Microbiol.* 2007;73:586–593.
29. Laspidou CS, Rittmann BE. A unified theory for extracellular polymeric substances, soluble microbial products, and active and inert biomass. *Water Res.* 2002;36:2711–2720.
30. Laspidou CS, Rittmann BE. Non-steady state modeling of extracellular polymeric substances, soluble microbial products, and active and inert biomass. *Water Res.* 2002;36:1983–1992.
31. Gujer W, Henze M, Mino T, van Loosdrecht MCM. Activated sludge model NO. 3. *Water Sci Technol.* 1999;39:183–193.
32. Reichert P. Aquasim 2.0-User Manual, Computer Program for the Identification and Simulation of Aquatic Systems; EAWAG: Dübendorf, Switzerland, 1998 (ISBN 3 906484 16 5).
33. de Kreuk MK, Picioreanu C, Hosseini M, Xavier JB, van Loosdrecht MCM. Kinetic model of a granular sludge SBR—influences on nutrient removal. *Biotechnol Bioeng.* 2007;97:801–815.
34. Beun JJ, Heijnen JJ, van Loosdrecht MCM. N-removal in a granular sludge sequencing batch airlift reactor. *Biotechnol Bioeng.* 2001; 75:82–92.
35. Wanner O, Reichert P. Mathematical modelling of mixed-culture bioflms. *Biotechnol Bioeng.* 1996;49:172–184.
36. Sin G, Guisasola A, de Pauw DJW, Baeza JA, Carrera J, Vanrolleghem PA. A new approach for modelling simultaneous storage and growth processes for activated sludge systems under aerobic conditions. *Biotechnol Bioeng.* 2005;92:600–613.
37. Karahan O, van Loosdrecht MCM, Orhon D. Modeling the utilization of starch by activated sludge for simultaneous substrate storage and microbial growth. *Biotechnol Bioeng.* 2006;94:43–53.
38. Nichols CAM, Garon S, Bowman JP, Raguenes G, Guezennec J. Production of exopolysaccharides by Antarctic marine bacterial isolates. *J Appl Microbiol.* 2004;96:1057–1066.
39. Qin L, Liu QS, Yang SF, Tay JH, Liu Y. Stressful conditions-induced production of extracellular polysaccharides in aerobic granulation process. *Civil Eng Res.* 2004;17:49–51.
40. Ahn YT, Choi YK, Jeong HS, Chae SR, Shin HS. Modeling of extracellular polymeric substances and soluble microbial products production in a submerged membrane bioreactor at various SRTs. *Water Sci Technol.* 2006;53:209–216.
41. Aquino SF, Stuckey DC. Integrated model of the production of soluble microbial products (SMP) and extracellular polymeric substances (EPS) in anaerobic chemostats during transient conditions. *Biochem Eng J.* 2008;38:138–146.
42. Ramesh A, Lee DJ, Hong SG. Soluble microbial products (SMP) and soluble extracellular polymeric substances (EPS) from wastewater sludge. *Appl Microbiol Biotechnol.* 2006;73:219–225.
43. Horn H, Neu TR, Wulkow M. Modelling the structure and function of extracellular polymeric substances in biofilms with new numerical techniques. *Water Sci Technol.* 2001;43:121–127.

*Manuscript received Jun. 9, 2008, revision received Nov. 6, 2008, and final revision received Feb. 25, 2009.*